Advances in Astronomy and Space Physics, **2**, 56-59 (2012)

The distribution of dark matter and intracluster gas in galaxy clusters

Iu. Babyk[1,4]*, *O. Melnyk*[2,3], *A. Elyiv*[3,4]

[1]Faculty of Physics, Taras Shevchenko National University of Kyiv, Glushkova ave., 4, 03127, Kyiv, Ukraine
[2]Astronomical Observatory, Taras Shevchenko National University of Kyiv, Observatorna St., 3, 04053, Kyiv, Ukraine
[3]Institut d'Astrophysique et de Géophysique, Université de Liège, 4000, Liège, Belgium
[4]Main Astronomical Observatory of NAS of Ukraine, Akademika Zabolotnoho St., 27, 03680, Kyiv, Ukraine

We present the temperature radial profiles of intracluster gas, and the radial profiles of density and mass for dark matter and intracluster gas for five galaxy clusters: Abell 1413, Abell 1204, Abell 2744, Abell 223 and CL 0024+17 observed by Chandra X-ray Observatory. These profiles were obtained based on the well-established fact, that the X-ray observed surface brightness of clusters are described well with the Navarro-Frenk-White density profile of the underlying dark matter distribution. We have found that density and mass profiles for all considered clusters have the same shape. Temperatures, masses and densities of these clusters lie within the ranges $5-10$ keV, $\sim 10^{14}-10^{15} M_{\odot}$ and $\sim 10^{-23}-10^{-25}$ kg/m^3 respectively. We also determined the values of R_{200} and M_{200} for the clusters and estimated the fraction of gas and dark matter in total mass of each cluster to be $\sim 10-20\%$ and $\sim 80-90\%$ respectively.

Key words: galaxies: clusters: intracluster medium; X-rays: galaxies: clusters

INTRODUCTION

Clusters of galaxies are the largest virialized structures in the Universe. Clusters consist of galaxies, hot ($\sim 10^7$ K) gas and dark matter and are ideal laboratories for cosmological studies as they were formed in the recent cosmological epoch (from $z \sim 2$ up to the present time) [2]. In this paper we used X-ray properties of hot gas for studing the mass distribution in five galaxy clusters.

Thoughout the paper we adopt $H_0 = 73$ km/s/Mpc, $\Omega_m = 0.27$ and $\Omega_\Lambda = 0.73$.

DATA REDUCTION

We used `CIAO` [4] software package version 4.2 for data reduction of five galaxy clusters (main characteristics of these clusters are presented in Table 1). We detected and removed all point sources from matrix. The each cluster image was split onto concentric annuli. Then we extracted the spectra from each region and fitted them using `Xspec` software package version 12.6 [1]. For the fitting we chose `WABS`×`MEKAL` model. `WABS` describes the Galactic absorption [3] which is different for each cluster (see Table 1). `MEKAL` is a model describing emission spectrum of hot diffuse plasma [5, 6, 7]. Firstly we fixed all the parameters and found the value of the temperature (kT) in each region (see Table 1). Then fixing the average temperature for each cluster we found the parameter *norm* of the `MEKAL` model. This parameter is proportional to the electron and proton concentrations ($\sim \frac{10^{-14}}{4\pi(D_a(1+z))^2}\int n_e n_p dV$, [10]).

MODELLING

We used numerical simulations for reconstruction of the dark matter distribution in considered galaxy clusters. Our model assumes that the hot gas traces the cluster gravitational potential which is mainly caused by the dark matter distribution. In order to model the dark matter density profile of a cluster, we used the Navarro-Frenk-White (NFW) [8] profile as one of the most successful representation of dark matter distribution:

$$\rho(r) = \frac{\rho_0}{\left(\frac{r}{r_s}\right)\left(1+\frac{r}{r_s}\right)^2}, \qquad (1)$$

where ρ_0 is the characteristic density of the dark matter, r_s is the core radius of the dark matter halo. A massive dark matter halo is characterized by a gravitational field which determines the shape of the hot

*babikyura@gmail.com

Table 1: The characteristics of our sample of galaxy clusters.

Cluster	z	$ObsID$	t_{exp}, ks	Instrument	$N_H, 10^{20} cm^{-2}$	kT, keV
Abell 223	0.21	4967	45.6	ACIS-I	2.2	$5.01^{+0.85}_{-0.91}$
Abell 1204	0.17	2205	23.9	ACIS-I	1.4	$4.84^{+1.93}_{-1.34}$
Abell 1413	0.14	537	9.34	ACIS-I	2.19	$8.07^{+2.28}_{-2.02}$
Abell 2744	0.31	2212	25.14	ACIS-S	1.62	$9.82^{+0.43}_{-0.41}$
CL0024+17	0.39	929	40.34	ACIS-S	4.22	$4.35^{+0.51}_{-0.44}$

gas halo. The gravitational potential ϕ can be found from:

$$\frac{d\phi}{dr} = G\frac{M(<r)}{r^2}. \quad (2)$$

All the following computations were done assuming the hydrostatic equilibrium condition of the X-ray emitting gas in galaxy clusters and isothermal condition $T_c = const$. The hydrostatic equilibrium condition can be written in the following form:

$$\bigtriangledown P = -\rho_g \bigtriangledown \phi(r), \quad (3)$$

where P and ρ_g are the pressure and the density of gas, respectively. Since the hot gas density is low enough, using the ideal gas law we obtained equation for the unknown gas density distribution:

$$\frac{\bigtriangledown \rho_g}{\rho_g} = -\bigtriangledown \phi(r)\frac{\mu m_p}{kT_g}. \quad (4)$$

For the reconstruction of a hot gas density field of galaxy clusters we had to solve numerically the system of differential equations.

RESULTS

We reconstructed the parameters of the dark matter distribution by fitting the observational X-ray data with our modelling results. We found the best-fit values for parameters ρ_0 and r_s, calculated the cluster potential, and using it determined the distribution of the hot gas. Then we used these results for determination of the surface brightness profiles and compared them with the observed ones (see Fig. 1). For the verification of our results we used the χ^2 test.

We used two free parameters ρ_0 and r_s for reconstruction of the density and mass (see Fig. 2–6) distribution for the dark matter and the gas. We also built the integrated total mass profile for each cluster (see Fig. 7) and scaled mass profiles of all clusters (see Fig. 8). The mass was scaled to M_{200}, which is the mass corresponding to a density contrast of $\delta = 200$, i. e. the mass contained in a sphere of radius R_{200}, which encompasses a mean density in 200 times. The critical density at the cluster redshift is determined as

$$\rho_{cr}(z) = \frac{3E^2(z)H_0^2}{8\pi G}, \text{ where } E^2(z) = \Omega_m(1+z)^3+\Omega_\Lambda.$$

This sphere is found to be in agreement with a virialized part of clusters [9]. The masses M_{200}, radii R_{200} and the fraction of the dark matter in the total mass for each cluster are presented in Table 2.

CONCLUSIONS

We have obtained the total mass of five clusters of galaxies: $4.44^{+0.45}_{-0.61} \cdot 10^{14} M_\odot$, $3.05^{+0.33}_{-0.23} \cdot 10^{14} M_\odot$, $8.61^{+0.49}_{-0.46} \cdot 10^{14} M_\odot$, $22.20^{+1.30}_{-1.20} \cdot 10^{14} M_\odot$ and $3.51^{+0.38}_{-0.47} \cdot 10^{14} M_\odot$ for A223, A1204, A1413, A2744 and CL0024+17, respectively. We determined the fraction of the dark matter in the total mass of the galaxy clusters: 0.85, 0.83, 0.84, 0.84 and 0.88 for A223, A1204, A1413, A2744 and CL0024+17, respectively. We conclude that NFW profile is a good representation for five of total mass profiles.

ACKNOWLEDGEMENTS

We thank for all members of Chandra collaboration for such an excellent X-ray data of galaxy clusters. We are also thankful to the anonymous referee for helpful comments and suggestions.

REFERENCES

[1] Arnaud K. 1996, 'Astronomical Data Analysis Software and Systems V', A.S.P. Conference Series, eds.: Jacoby G. H. & Barnes J., 101, 17
[2] Arnaud M., Pratt G. & Pointecouteau E. 2004, Memorie della Società Astronomica Italiana, 75, 529
[3] Dickey J. & Lockman F. 1990, ARA&A, 28, 215
[4] Fruscione A., McDowell J. C., Allen G. E. et al. 2006, Observatory Operations: Strategies, Processes, and Systems, eds.: Silva D. R. & Doxsey R. E., Proc. of the SPIE, 6270, 62701V
[5] Kaastra J. S. 1992, 'An X-Ray Spectral Code for Optically Thin Plasmas' (Internal SRON-Leiden Report, updated version 2.0)
[6] Liedahl D. A., Osterheld A. L. & Goldstein W. H. 1995, ApJ, 438, L115
[7] Mewe R., Lemen J. R. & van den Oord G. H. J. 1986, A&AS, 65, 511
[8] Navarro J. F., Frenk C. S. & White S. D. M. 1996, ApJ, 462, 563
[9] Pointecouteau E., Arnaud M. & Pratt G. W. 2005, Advances in Space Research, 36, 659
[10] Vikhlinin A., Forman W. & Jones C. 1999, ApJ, 525, 47

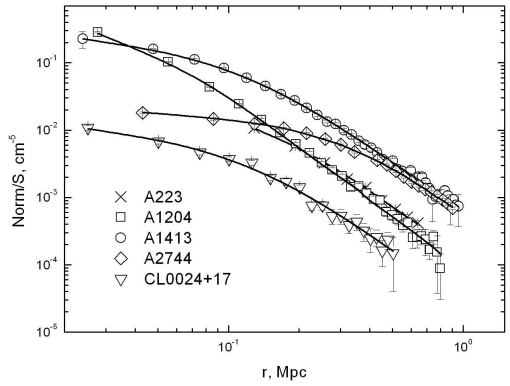

Fig. 1: Surface brightness profiles for all galaxy clusters.

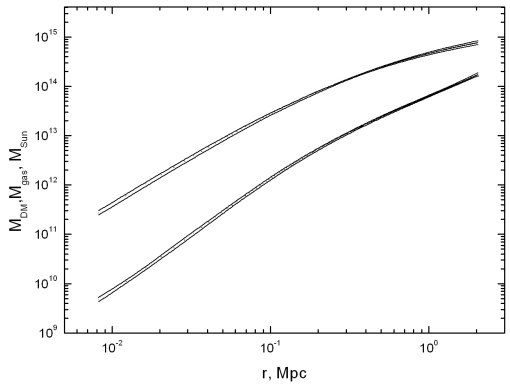

Fig. 2: The integrated mass profiles for the dark matter (upper curve) and gas (lower curve) of A1413.

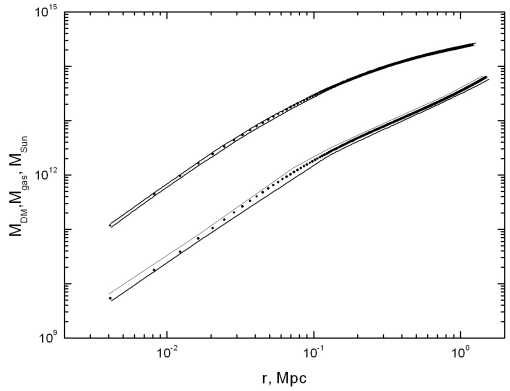

Fig. 3: The integrated mass profiles for the dark matter (upper curve) and gas (lower curve) of A1204.

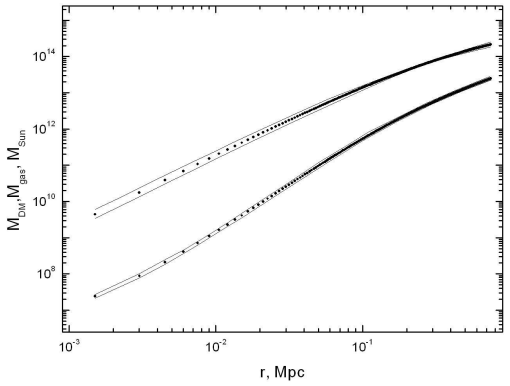

Fig. 4: The integrated mass profiles for the dark matter (upper curve) and gas (lower curve) of A223.

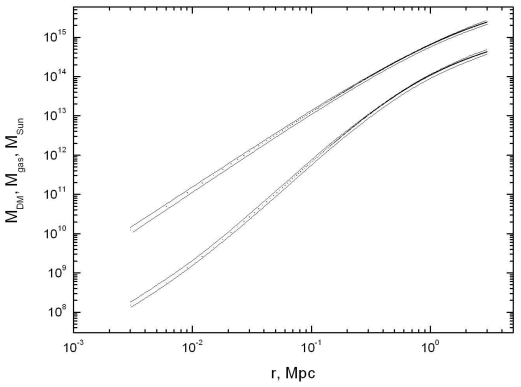

Fig. 5: The integrated mass profiles for the dark matter (upper curve) and gas (lower curve) of A2744.

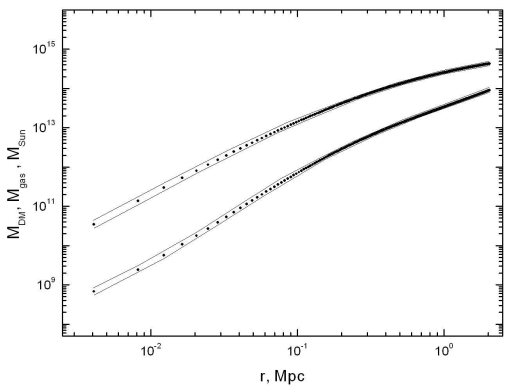

Fig. 6: The integrated mass profile for the dark matter (upper curves) and gas (lower curves) of CL0024+17 .

Table 2: Results for the NFW mass profile fitting.

Cluster	R_{200}, Mpc	M_{200}, $10^{14} M_{\odot}$	M_{DM200}/M_{200}
Abell 223	$1.44^{+0.26}_{-0.21}$	$4.44^{+0.45}_{-0.61}$	0.85
Abell 1204	$1.28^{+0.44}_{-0.26}$	$3.05^{+0.33}_{-0.23}$	0.83
Abell 1413	$1.83^{+0.66}_{-0.57}$	$8.61^{+0.49}_{-0.46}$	0.84
Abell 2744	$2.38^{+0.13}_{-0.12}$	$22.20^{+1.30}_{-1.20}$	0.84
CL0024+17	$1.24^{+0.12}_{-0.17}$	$3.51^{+0.38}_{-0.47}$	0.88

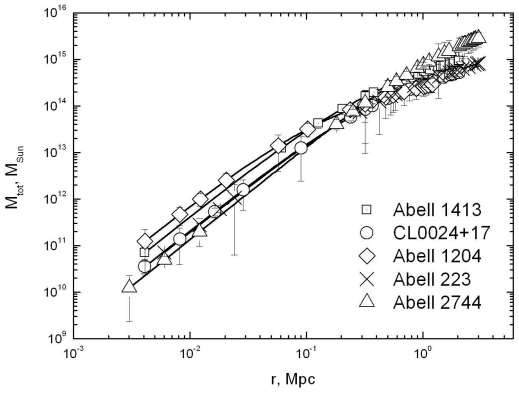

Fig. 7: The integrated total mass profiles. The solid lines represent the best fitting by NFW profiles.

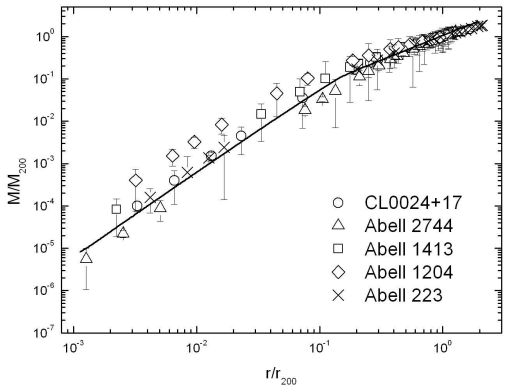

Fig. 8: The mass is scaled to M_{200} and the radius to R_{200}, both values being derived from the best fitting NFW model. The solid black line corresponds to the mean scaled NFW profile.